High Light Acclimation in the Secondary Plastids Containing Diatom *Phaeodactylum tricornutum* is Triggered by the Redox State of the Plastoquinone Pool[1][W][OA]

Bernard Lepetit*, Sabine Sturm, Alessandra Rogato, Ansgar Gruber[2], Matthias Sachse, Angela Falciatore, Peter G. Kroth, and Johann Lavaud

Littoral Environnement et Sociétés, Unité Mixte de Recherche 7266, Centre National de la Recherche Scientifique-University of La Rochelle, Institute for Coastal and Environmental Research, 17000 La Rochelle, France (B.L., J.L.); Universität Konstanz, Plant Ecophysiology, 78457 Konstanz, Germany (S.S., A.G., M.S., P.G.K.); Génomique des Microorganismes, Unité Mixte de Recherche 7238, Centre National de la Recherche Scientifique-Université Pierre et Marie Curie, 75006 Paris, France (A.R., A.F.); and Institute of Genetics and Biophysics, A. Buzzati-Traverso, Consiglio Nazionale delle Ricerche, 80131 Naples, Italy (A.R.)

In diatoms, the process of energy-dependent chlorophyll fluorescence quenching (qE) has an important role in photoprotection. Three components are essential for qE: (1) the light-dependent generation of a transthylakoidal proton gradient; (2) the deepoxidation of the xanthophyll diadinoxanthin (Dd) into diatoxanthin (Dt); and (3) specific nucleus-encoded antenna proteins, called Light Harvesting Complex Protein X (LHCX). We used the model diatom *Phaeodactylum tricornutum* to investigate the concerted light acclimation response of the qE key components LHCX, proton gradient, and xanthophyll cycle pigments (Dd+Dt) and to identify the intracellular light-responsive trigger. At high-light exposure, the up-regulation of three of the *LHCX* genes and the de novo synthesis of Dd+Dt led to a pronounced rise of qE. By inhibiting either the conversion of Dd to Dt or the translation of *LHCX* genes, qE amplification was abolished and the diatom cells suffered from stronger photoinhibition. Artificial modification of the redox state of the plastoquinone (PQ) pool via 3-(3,4-dichlorophenyl)-1,1-dimethylurea and 5-dibromo-6-isopropyl-3-methyl-1,4-benzoquinone resulted in a disturbance of Dd+Dt synthesis in an opposite way. Moreover, we could increase the transcription of two of the four *LHCX* genes under low-light conditions by reducing the PQ pool using 5-dibromo-6-isopropyl-3-methyl-1,4-benzoquinone. Altogether, our results underline the central role of the redox state of the PQ pool in the light acclimation of diatoms. Additionally, they emphasize strong evidence for the existence of a plastid-to-nucleus retrograde signaling mechanism in an organism with plastids that derived from secondary endosymbiosis.

Diatoms are eukaryotic microalgae found in any aquatic habitat. They contribute to the global primary production to a similar extent as terrestrial tropical rain forests and grasslands (Geider et al., 2001). As such, they are at the onset of most marine and freshwater food webs (Armbrust, 2009). Because of their ecological importance, the genomes of several diatom species have meanwhile been sequenced and are publicly available (Tirichine and Bowler, 2011). Especially the physiological studies at the molecular level of the diatoms *Thalassiosira pseudonana* and *Phaeodactylum tricornutum* revealed a plethora of unique features (Wilhelm et al., 2006; Armbrust, 2009; Bowler et al., 2010). Some of these features arise from the chimerical origin of the genome, which is due to horizontal gene transfer from bacteria and to the evolution of the diatom chloroplasts via secondary endosymbiosis (Bowler et al., 2010). After each endosymbiotic event, gene transfer from the endosymbiont to the nucleus occurred, permanently modifying the genome composition of the host cell. Still, the diatom chloroplast genome retained a small amount of approximately 130 protein-encoding genes (Oudot-Le Secq et al., 2007). As a further consequence of secondary endosymbiosis, diatom plastids are surrounded by an envelope of four membranes reflecting the endosymbiotic origin of these organelles (Green, 2011).

Gene transfer from the chloroplast into the nucleus is common to all eukaryotic phototrophs. Because many of the plastid-localized proteins are encoded by

[1] This work was supported by the German Academic Exchange Service (postdoctoral grant to B.L.), the Centre National de la Recherche Scientifique and the French consortium Contrat de Projets État-Région Littoral (grants to J.L. and B.L.), the Deutsche Forschungsgemeinschaft (grant nos. LA–2368/2–1 to J.L. and KR–1661/7–1 to P.G.K.), the Agence Nationale de la Recherche (grant no. DiaDomOil ANR–12–BIME–0005–03 to A.F.), and the Universität Konstanz.

[2] Present address: Department of Biochemistry and Molecular Biology, Dalhousie University, Halifax, Nova Scotia, Canada B3H 4R2.

* Corresponding author; e-mail bernard.lepetit@univ-lr.fr.

The author responsible for distribution of materials integral to the findings presented in this article in accordance with the policy described in the Instructions for Authors (www.plantphysiol.org) is: Bernard Lepetit (bernard.lepetit@univ-lr.fr).

[W] The online version of this article contains Web-only data.

[OA] Open Access articles can be viewed online without a subscription.

www.plantphysiol.org/cgi/doi/10.1104/pp.112.207811

the nuclear genome and because most of the plastid protein complexes are chimeras of nucleus- and plastid-encoded proteins, both the plastidic and nuclear gene expression as well as the respective protein import into the plastids require a fine-tuned regulation (Allen et al., 2011). Thus, anterograde (nucleus-to-plastid) and retrograde (plastid-to-nucleus) signaling pathways are widespread processes to coordinate gene expression in green algae and land plants (Kleine et al., 2009). The control of photosynthetic gene expression and enzyme activity is coordinated by a number of molecular triggers, including photosynthetic metabolites, hormones, chlorophyll and carotenoid biosynthesis precursors, photoreceptors, stress-generated reactive oxygen species (ROS), and soluble redox-active compounds (Kleine et al., 2009; Pfannschmidt, 2010; Foyer et al., 2012). A further important signaling trigger is the redox state of the plastoquinone (PQ) pool of the plastid electron transport chain. Besides its well-known involvement in the irradiance-dependent regulatory process of state transitions in green microalgae and plants, it has a key role for the regulation of both chloroplast and nuclear gene expression under light-changing conditions (Pfannschmidt, 2003). In diatoms, the involvement of photoreceptors in photosynthetic regulatory processes has been revealed recently (Depauw et al., 2012), while redox regulation via thioredoxins seems to be of minor importance for the regulation of the Calvin cycle (Kroth et al., 2008), even if thioredoxins may control the activity of carboanhydrases in the pyrenoid (Kikutani et al., 2012). The redox state of the PQ pool is of crucial importance in several photosynthetic regulatory processes, such as the PSII electron cycle (Onno Feikema et al., 2006; Lavaud et al., 2007), nonphotochemical fluorescence quenching (NPQ; Lavaud, 2007; Lavaud et al., 2007), and chlororespiration (Caron et al., 1987; Dijkman and Kroon, 2002; Grouneva et al., 2009). The dynamics of the PQ pool redox state as a function of light intensity differ between diatom species and between diatoms and land plants (Ruban et al., 2004; Lavaud, 2007; Materna et al., 2009). So far, no evidence for an involvement of the PQ pool in redox signaling in diatoms has been published.

Diatoms possess an outstanding capacity to tolerate light fluctuations regularly punctuated by excess light exposure, which might be one of the reasons for their ecological success (Brunet and Lavaud, 2010). The central mechanism for the fast regulation of photochemistry under changing light conditions is NPQ. It takes place in the light-harvesting complex antennae (LHC) of PSII, where excessively absorbed light energy is dissipated as heat (Li et al., 2009; Ruban et al., 2012). In diatoms, the most important part of NPQ is the energy-dependent chlorophyll fluorescence quenching (qE), while photoinhibitory quenching is low, and state-transition quenching does not exist at all (Goss and Jakob, 2010). qE requires the irradiance-dependent establishment of a transthylakoidal proton gradient (ΔpH) and the conversion of the xanthophyll diadinoxanthin (Dd) into diatoxanthin (Dt) in the presence of a ΔpH (Goss and Jakob, 2010). Together with the reverse reaction in the absence of the ΔpH, this process is called the "xanthophyll cycle" and is equivalent to the violaxanthin, antheraxanthin, and zeaxanthin xanthophyll cycle in land plants (Jahns and Holzwarth, 2012). Furthermore, the presence of LHCX proteins is essential (Bailleul et al., 2010). In addition to LHCX, diatoms contain other members of the LHC protein superfamily, like LHCF, which constitutes the peripheral light-harvesting complex, and LHCR, which is tightly linked with PSI and whose function remains to be elucidated (Lepetit et al., 2012). Located in the plastids, the enzymes for the interconversion of the xanthophyll cycle pigments Dd+Dt, the Dd deepoxidases and the Dt epoxidases (Coesel et al., 2008; Lohr, 2011), as well as the LHCX proteins (Bowler et al., 2008; Zhu and Green, 2008; Engelken et al., 2012) are encoded in the nucleus. Dd+Dt and LHCX have been shown to be synthesized de novo during prolonged high-light stress (Olaizola et al., 1994; Bailleul et al., 2010; Zhu and Green, 2010). The de novo synthesis of Dd+Dt does not necessarily lead to higher NPQ (Lavaud et al., 2004; Schumann et al., 2007), but it can enhance the antioxidant activity within the thylakoid membranes (Lepetit et al., 2010). Nevertheless, reduced expression of the gene encoding the Dd deepoxidase clearly leads to both lower Dt synthesis and qE (Lavaud et al., 2012). Overexpression or underexpression of LHCX1 promotes higher or lower qE, respectively, and the up-regulation of LHCX2 and LHCX3 might confer more efficient photoprotection (Bailleul et al., 2010). In this study, we monitored the changes of Dd+Dt and LHCX during prolonged high-light exposure and the subsequent low-light exposure. Because light stress creates an increased reduction of the electron transport chain, we tested the possible involvement of the redox state of the PQ pool in the qE acclimation response using different light conditions and inhibitor treatments. By identifying a link between the redox state of the PQ pool and the regulation of the amount of the qE key players LHCX and Dd+Dt pigments, we deliver a so far missing piece of evidence for plastid-to-nucleus retrograde signaling in diatoms.

RESULTS

Expression of *LHCX* Genes under Different Light Conditions

LHCX gene expression was studied in *P. tricornutum* cells that had been cultured for 33 h in darkness, darkness/low light (LL; 40 μmol photons m^{-2} s^{-1}), or darkness/medium low light (mHL; 750 μmol photons m^{-2} s^{-1}). Except for the cells kept in the dark, the standard 16/8-h day/night rhythm was maintained. In prolonged dark conditions, *LHCX4* gene expression showed a significant increase during the daytime, while gene expression of *LHCX2* and *LHCX3*

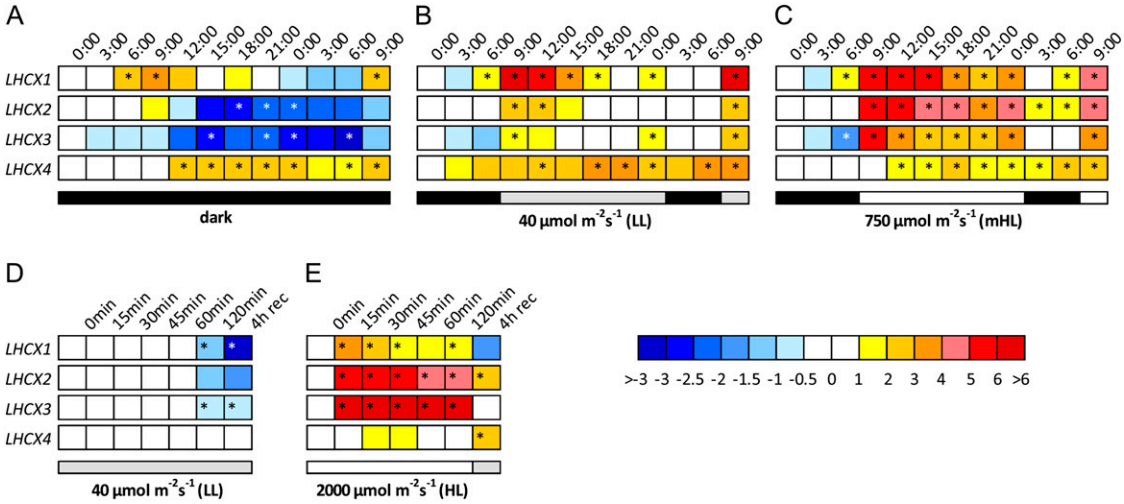

Figure 1. *LHCX* transcription levels in different light regimes. Expression ratios are given in $\log_2$-transformed values as indicated by the color bar and represent relative amounts with reference to *18S* gene expression. All levels were normalized to the respective initial value and represent means of four independent measurements. Asterisks represent significant changes at $P < 0.05$ (Pairwise Fixed Reallocation Randomization Test performed by REST). A to C, A 33-h experiment with darkness all the time (A), 40 μmol photons m^{-2} s^{-1} illumination (LL) from 8 AM until 12 AM (B), and 750 μmol photons m^{-2} s^{-1} illumination (mHL) from 8 AM until 12 AM (C). D and E, A 6-h experiment with LL illumination all the time (D) and 2,000 μmol photons m^{-2} s^{-1} illumination (HL) for the first 2 h followed by 4 h of LL recovery (E).

decreased (Fig. 1A). At 9 AM, after light had normally been switched on, the transcript level of *LHCX1* reached its maximum, after which it declined to increase again at the same time the next day. This rhythmic diurnal expression suggests the presence of a circadian regulation. LL conditions had a pronounced effect on the expression of *LHCX1*, *LHCX2*, and *LHCX3* (Fig. 1B). The two latter genes were slightly but significantly induced until noon, while *LHCX1* was highly up-regulated. mHL conditions strongly increased the expression of *LHCX2* and *LHCX3* (Fig. 1C). During the following night, the respective amounts of mRNA almost reached their initial level, indicating a fast regulation of transcript increase and decrease. The extra light intensity at mHL conditions compared with LL also resulted in an increase of *LHCX1* transcription, albeit to a lesser extent. *LHCX4* did not show any differences regarding transcription at both light treatments compared with cells kept in the dark.

In order to evaluate the effect of a high-light (HL) exposure equivalent to full sunlight in nature, the cells were exposed to 2,000 μmol photons m^{-2} s^{-1} (Long et al., 1994) for 2 h, and their recovery from HL stress was recorded during a subsequent LL exposure of 4 h. In this case, the transcription of *LHCX1*, *LHCX2*, and *LHCX3* was up-regulated while *LHCX4* appeared to be light insensitive (Fig. 1E). In contrast to cells grown at mHL conditions, *LHCX3* was the most strongly up-regulated gene (more than 100-fold), followed by *LHCX2* and *LHCX1*. After 4 h of recovery at LL, *LHCX3* reached its initial transcript level, indicating an extremely rapid up- and down-regulation. The reduction of transcripts was slower for *LHCX2*, while *LHCX1* transcripts even decreased below their initial level because of the daily regulation pattern.

Changes of Pigments and NPQ during mHL and HL Treatments

During the mHL exposure (16 h), no alterations were observed regarding the amounts of chlorophyll *c* and β-carotene per chlorophyll *a* (Chl *a*; Fig. 2A). The fucoxanthin (Fx) content per Chl *a* increased just after the onset of light and then slightly decreased. Pigments of the violaxanthin cycle, which were observed by Lohr and Wilhelm (1999), could not be recorded under our experimental conditions. The Dd+Dt concentration increased almost 4-fold (Fig. 2A), and the Dt amount became higher than Dd. Remarkably, the Dd+Dt pool size kept scaling up during the first 3 h of darkness and did not decrease during the resting night period. After HL treatment (2 h), we detected an equally strong increase of Dd+Dt (Figs. 2B and 3A). The de novo synthesis of Dd+Dt started approximately 30 min after the light onset, as reported before (Lavaud et al., 2004), and rapidly declined within the 4 h of LL recovery. In contrast, during dark recovery, the amount of Dd+Dt remained stable (Fig. 3A). Also, we did not observe major differences in the amount of all other pigments, indicating a rather independent synthesis and degradation of Dd+Dt from Fx and β-carotene. Interestingly, the epoxidation of Dt to Dd occurred rapidly and almost completely during the recovery period, no matter whether LL or darkness was employed (Fig. 3B).

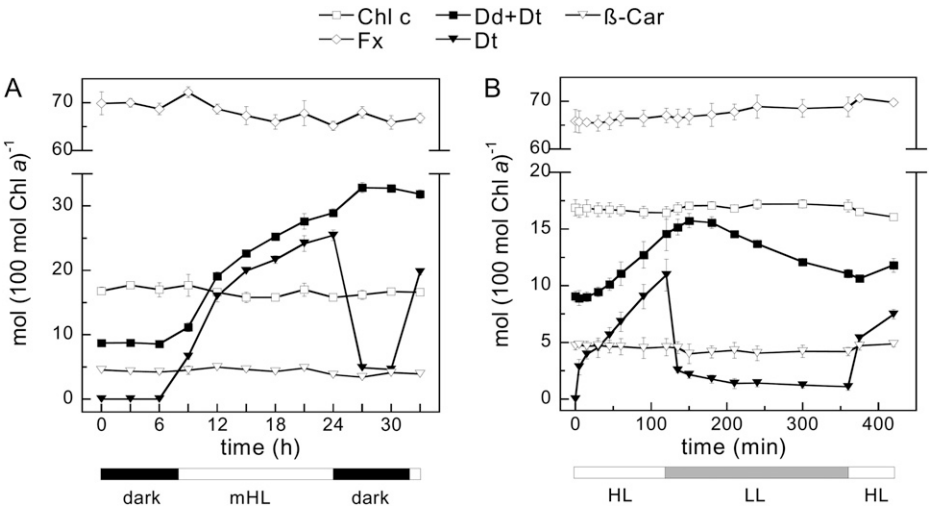

Figure 2. Pigment evolution during the mHL (A) and HL (B) experiments. In A, the recovery period was performed at darkness, while in B, recovery was monitored at LL conditions. After 4 h of recovery from HL, cells were again exposed to 1 h of HL treatment. Values are means of three (A) and five (B) independent experiments ± SD. β-Car, β-Carotene.

An inverse relationship was observed between NPQ and the effective PSII quantum yield (F_v/F_m) during the mHL exposure. The NPQ increased, albeit with a much lower slope during the second half of the light treatment, while F_v/F_m concomitantly decreased (Supplemental Fig. S3). The NPQ did not relax completely during the dark recovery period. A strong increase of NPQ was also observed during the HL experiments (Fig. 3C). Its maximal value was lower than during the mHL treatment (1.65 versus 2.75),

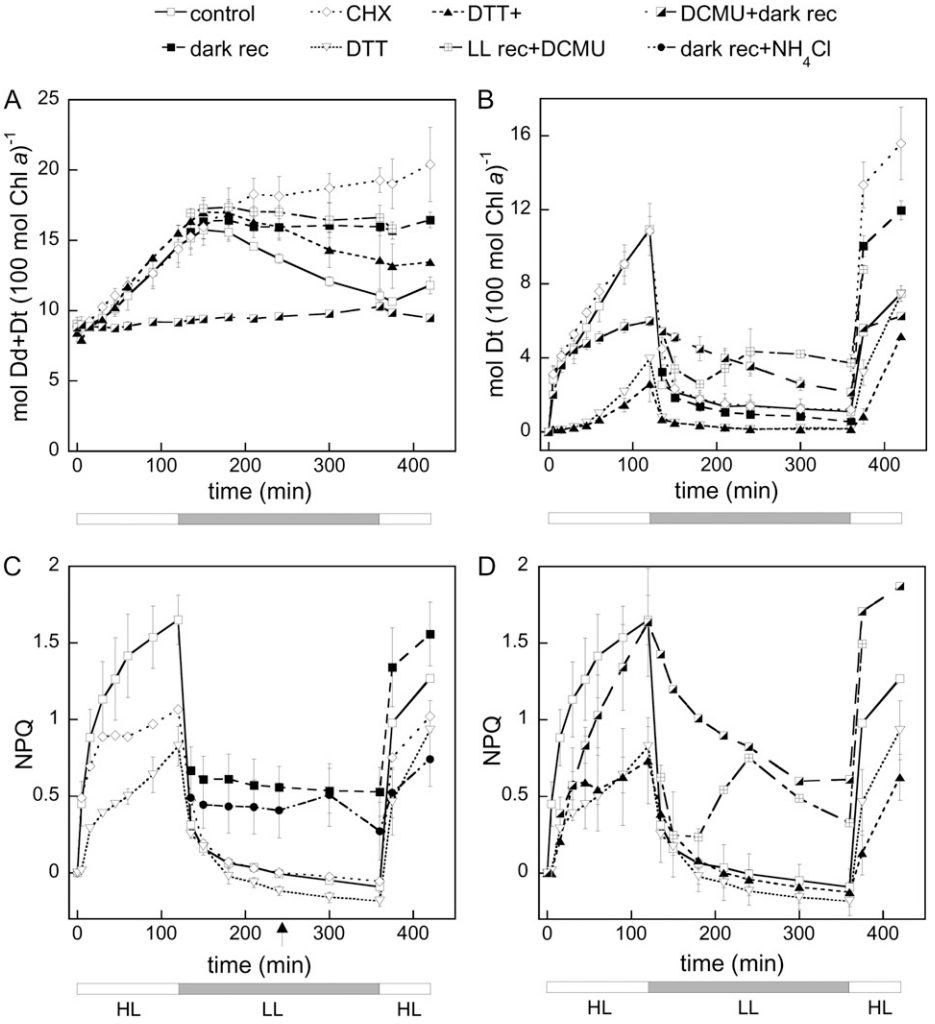

Figure 3. Dd+Dt (A) and Dt (B) content and NPQ (C and D) during 2 h of HL treatment, 4 h of LL recovery, and subsequently 1 h of HL treatment. Control, Cultures without inhibitors; dark rec, after 2 h of HL exposure, 4 h of darkness followed instead of 4 h of LL; CHX, cultures were incubated with 2 μg mL^{-1} CHX for 45 min before starting the experiment; DTT, cultures were incubated with DTT (500 μM) for 15 min before starting the experiment; DTT+, DTT (500 μM) was added additionally every 20 min during the HL treatment and 20 min before the second HL treatment; LL rec+DCMU, DCMU (10 μM) was added before starting the LL recovery period; DCMU+dark rec, DCMU (10 μM) was added 10 min before light exposure, and recovery was performed in darkness; dark rec+NH_4CL, recovery was performed in darkness, and after 2 h of darkness, NH_4Cl (5 mM) was added (indicated with the arrow). Samples represent means of two to five independent experiments ± SD, except for the NPQ values of DCMU-treated samples during the recovery time, where only one experiment was performed.

which can be explained by the shorter light treatment (2 versus 16 h). NPQ completely relaxed during the LL recovery period but not in darkness (Fig. 3C). The addition of NH_4Cl, which usually relaxes NPQ efficiently in *P. tricornutum* (Goss et al., 2006), could not reduce the NPQ persisting in the dark (Fig. 3C).

The NPQ/Dt relationship reflects the Dt quenching efficiency (Lavaud et al., 2002a, 2004), which in the mHL experiments showed a highly linear correlation ($r^2 = 0.98$) up to a threshold value of 20 mol Dt 100 mol^{-1} Chl *a* at the 3 PM time point (Supplemental Fig. 4A). Beginning at 6 PM, the slope of the relationship strongly decreased. The respective values during the HL treatment yielded a strong linear correlation ($r^2 = 0.96$) up to 60 min and a threshold concentration of 7 mol Dt 100 mol^{-1} Chl *a*, while the slope of the relationship during the second hour of illumination dramatically dropped (Supplemental Fig. 4, A and B). Moreover, the values for the steep slopes of the NPQ/Dt relationships in mHL and HL were different (0.125 versus 0.218; Supplemental Fig. 4A).

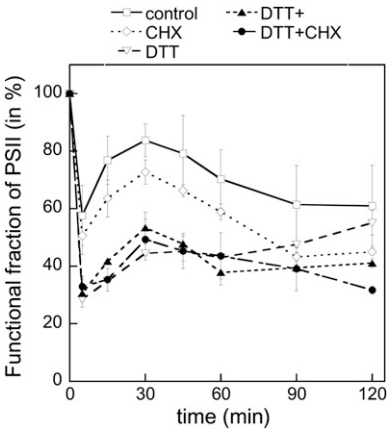

Figure 4. Functional fraction of PSII (in percentage) during 2 h of HL treatment as an indicator of PSII photoinactivation calculated by $1/F_o - 1/F_m$. The ratio $1/F_o - 1/F_m$ obtained before the start of the light treatment was taken as 100%. For definitions, see Figure 3. DTT+CHX, DTT (500 μM) and CHX (2 μg mL^{-1}) were added 15 and 45 min before light exposure, respectively.

Influence of Dithiothreitol and Cycloheximide on NPQ, Dd+Dt, and LHCX Synthesis

Because the photoacclimative responses were already fully activated during the 2 h of HL exposure, the inhibitor treatments were performed at these conditions. Dithiothreitol (DTT), an inhibitor of the deepoxidation reaction (Yamamoto and Kamite, 1972), had no effect on the increase of the Dd+Dt pool size (Fig. 3A, DTT+) but blocked the Dd deepoxidation during the first 30 min of illumination (Fig. 3B, DTT). Afterward, when the Dd+Dt pool size increased, a considerable amount of Dt was produced even in the presence of DTT. To exclude the possibility that the inhibitor effect is reduced after 30 min of HL, DTT was alternatively added every 20 min (Fig. 3B, DTT+). The supplementary DTT dose slowed down the Dt synthesis while not completely inhibiting it. As expected, both DTT treatments (DTT and DTT+) strongly inhibited the induction of NPQ (Fig. 3, C and D) and resulted in a dramatic decrease of the functional fraction of PSII (Fig. 4).

Cycloheximide (CHX) blocks the translation of nucleus-encoded genes on cytosolic 80S ribosomes and therefore does not influence gene translation in the organelles (Obrig et al., 1971; Setkov et al., 1992). As a matter of fact, while HL treatment induced the synthesis of nucleus-encoded LHCX2 and LHCX3 proteins (Fig. 5), as expected from the transcript level measurements (Fig. 1), the addition of CHX prevented it. In contrast, CHX had no inhibiting effect on the plastid-encoded PsbB protein; instead, a slightly increased amount of PsbB was detected, as observed before in other diatoms (Wu et al., 2011). We did not notice any differences in the amounts of LHCX1 after HL treatment. This might be due to either an oversaturation of the western blot because of the already rather high initial LHCX1 amount or a different regulation on the posttranslational level. Addition of CHX did not alter the de novo synthesis of Dd+Dt or the amount of Dt produced during HL exposure (Fig. 3, A and B), but it completely prevented the decrease of Dd+Dt during the LL recovery period, similar to the dark recovery experiments in the absence of the inhibitor. However, after 30 min of HL, CHX retarded a further increase of NPQ almost completely (Fig. 3C) and increased the degree of PSII photoinactivation, although not as pronounced as DTT (Fig. 4). As expected, we obtained the highest degree of photoinactivation by adding both CHX and DTT.

Only during the first 30 min of HL and CHX treatment did we find a highly linear correlation of Dt versus NPQ ($r^2 = 1$); thereafter, the slope dropped close to zero. The threshold concentration for Dt participating in NPQ decreased to a value of around 5 mol Dt 100 mol^{-1} Chl *a* (Supplemental Fig. 4B).

Effect of 3-(3,4-Dichlorophenyl)-1,1-Dimethylurea and 5-Dibromo-6-Isopropyl-3-Methyl-1,4-Benzoquinone on the Dd+Dt Pool Size

In diatoms, a chlororespiration process exists that influences the redox state of the PQ pool in the dark (Jakob et al., 1999; Dijkman and Kroon, 2002; Wilhelm et al., 2006; Grouneva et al., 2009). As we saw a clear difference in the Dd+Dt pool size during dark or LL recovery, 3-(3,4-dichlorophenyl)-1,1-dimethylurea (DCMU) was utilized to modify the PQ pool redox state. By binding to the secondary electron-accepting plastoquinone of PSII (Q_B), DCMU generates a reduced primary electron-accepting plastoquinone of PSII (Q_A) and an oxidized PQ pool (Trebst, 2007). Applied during the LL recovery conditions, DCMU prevented the decrease of the Dd+Dt pool (Fig. 3A), comparably to the dark recovery in the

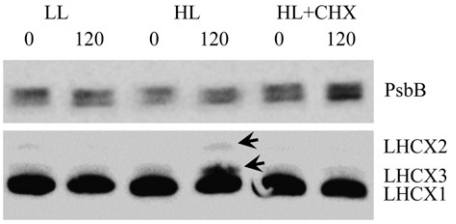

Figure 5. Western blot of LL-, HL-, and HL- + CHX-treated cultures. Indicated are the samples before (0) and after (120) 2 h of LL or HL treatment, respectively. A polyclonal LHCSR antibody of *C. reinhardtii* was employed, which detects all of the LHCX proteins. Arrows indicate LHCX2 and LHCX3, which can be distinguished from LHCX1 by their larger size. As a loading control, an antibody against the plastid-encoded PsbB (CP47) was applied.

absence of the inhibitor. On the other hand, DCMU induced a pronounced deepoxidation, probably due to the onset of cyclic electron transport around PSI (Fig. 3B). By applying DCMU directly at the beginning of the HL exposure (i.e. by mimicking LL conditions regarding the redox state of the PQ pool), no Dd+Dt pool size increase was observed (Fig. 3A), but again, a strong deepoxidation occurred (Fig. 3B). In order to verify these results, we used 5-dibromo-6-isopropyl-3-methyl-1, 4-benzoquinone (DBMIB), which usually shows the opposite effect compared with DCMU regarding the redox state of the PQ pool. DBMIB binds close to the plastoquinol-oxidizing Qo-site of the cytochrome b_6f complex and consequently induces a reduced PQ pool under LL, which hence mimics HL conditions (Kurisu et al., 2003; Trebst, 2007). Because this effect is known to depend on the concentration of DBMIB, we tested different amounts in order to define a suitable DBMIB concentration necessary to induce a reduced PQ pool following two main criteria: (1) a high F_v/F_m served as a proof that DBMIB does not bind to Q_B, which can occur at too-high concentrations (Vener et al., 1997); and (2) we checked for a reduced NPQ compared with the control because of the limited proton translocation at the cytochrome b_6f complex (Strzepek and Harrison, 2004). The suitable DBMIB concentration was defined to be 1 μM (Supplemental Fig. 5), which is consistent with concentrations used in green microalgae (Steinbrenner and Linden, 2003) and in land plants (Tullberg et al., 2000). One micromolar DBMIB at a light intensity of 100 μmol photons m^{-2} s^{-1} (LL_{100}) was sufficient to support a considerable electron flow from PSII to PSI while neither inducing any Dd deepoxidation nor any decrease of F_v/F_m (data not shown). DBMIB + LL_{100} led to a 20% increase of Dd+Dt in contrast to untreated cells (Fig. 6). A reduced PQ pool, therefore, could induce an HL response under LL conditions.

Effect of DCMU and DBMIB on LHCX Transcript Levels

The described DBMIB + LL_{100} HL-mimicking system was then applied for further analysis of *LHCX* transcript levels. While the LL_{100} treatment alone did not induce remarkable transcript changes in any of the *LHCX*, the addition of DBMIB caused a slight rise of the *LHCX1* transcript level (Fig. 7A) and a pronounced increase of *LHCX2* (20-fold after 60 min; Fig. 7B). In contrast, the amount of *LHCX3* transcripts did not change (Fig. 7C). Hence, for two of the three light-induced *LHCX*, gene expression was specifically stimulated by an increased reduction state of the PQ pool. The addition of DCMU during HL treatment did not produce the opposite effect of DBMIB, even when the light intensity was decreased to 500 μmol photons m^{-2} s^{-1} (Supplemental Fig. S6), most probably because the combined effect of HL and DCMU on photosynthesis was higher than the DCMU-generated artificial LL effect. Instead, we used DCMU during the DBMIB + LL_{100} treatment in order to stop the electron flow from PSII to cytochrome b_6f, relaxing the reduced PQ pool redox state. This abolished the effect of DBMIB on the transcript levels of *LHCX1* and *LHCX2* (Fig. 7, A and B) and demonstrated that DBMIB did not simply induce the transcription of these genes due to its presence per se but due to its effect on the redox state of the PQ pool. The light-insensitive *LHCX4* gene responded differently. Its transcription was slightly induced by the DBMIB + LL_{100} treatment (Fig. 7D), but it was neither abolished by the addition of DCMU nor increased during the HL + DCMU treatment (Supplemental Fig. S6). *LHCX4* apparently reacted specifically in the presence of DBMIB rather than to the changes of the redox state of the PQ pool itself.

DISCUSSION

The Role of Dt and LHCX in NPQ

The presented results strengthen previous findings whereupon LHCX1, LHCX2, and LHCX3, but

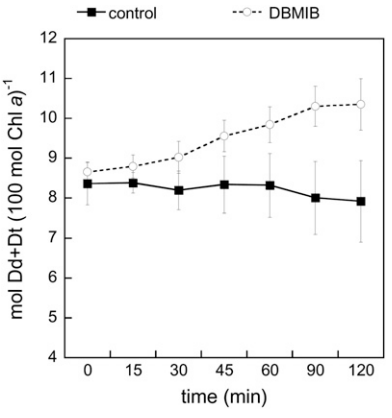

Figure 6. Evolution of the Dd+Dt pool size during illumination with LL_{100}. In these conditions, the Dt amount was less than 2% of the total Dd +Dt pool size in both experimental conditions. In the inhibitor treatment, 1 μM DBMIB was added 10 min before the start of the experiment. Depicted are mean values of four independent measurements ± SD.

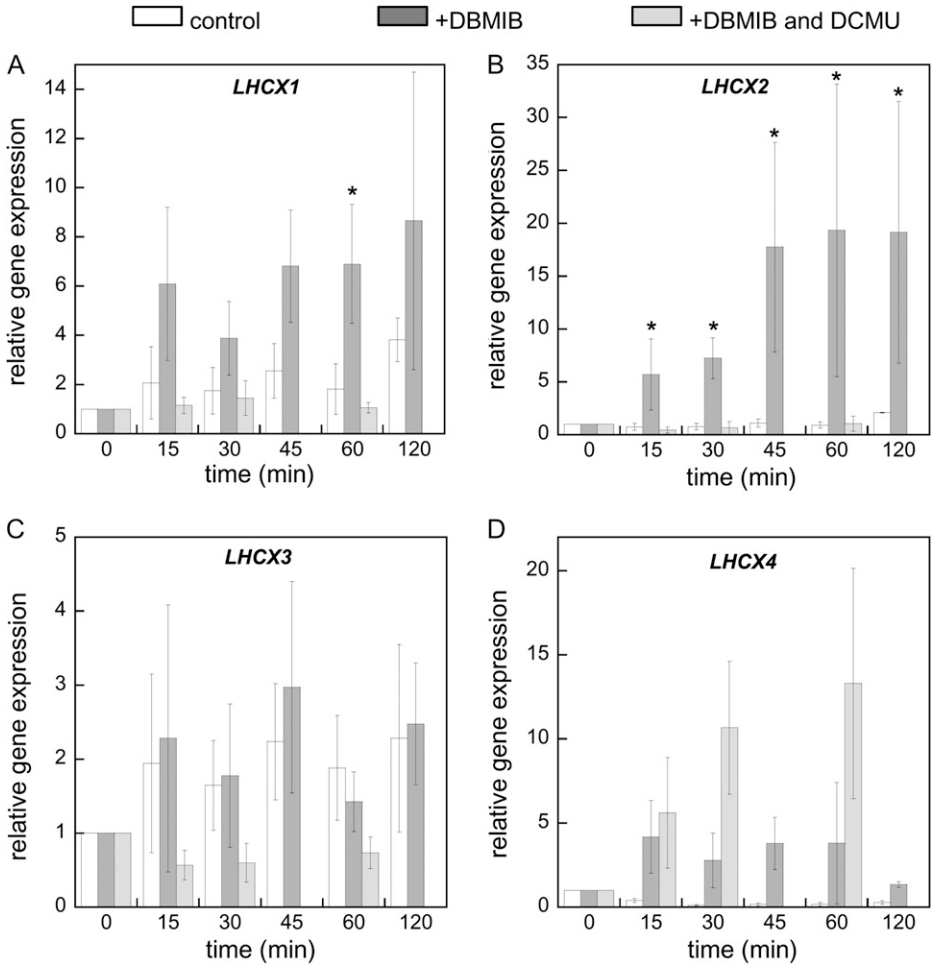

Figure 7. Relative gene expression of *LHCX1* (A), *LHCX2* (B), *LHCX3* (C), and *LHCX4* (D) during illumination with LL_{100}. Relative *LHCX* transcription levels with reference to *18S* gene expression were normalized to the initial amount. White bars, no chemical treatment; dark gray bars, 1 μM DBMIB was applied 10 min before the light treatment; light gray bars, in addition to DBMIB, 10 μM DCMU was applied 10 min before the light treatment. Analyses were performed at the indicated time points, and values represent means of three independent samples ± SD. Asterisks represent significant differences ($P < 0.05$; Pairwise Fixed Reallocation Randomization Test performed by REST) of the DBMIB-treated samples compared with the respective control samples and, when available, also compared with the respective DBMIB- + DCMU-treated samples. *LHCX4* was significantly upregulated in the presence of DBMIB compared with the control conditions at each time point. As this significance was abolished by comparing DBMIB-treated with DBMIB- + DCMU-treated samples, these are false-positive results; therefore, significance is also not indicated for time points 45 and 120 min.

not LHCX4, are involved in the photoacclimative/photoprotective response of diatoms (Nymark et al., 2009; Bailleul et al., 2010). The Pt4 strain studied here shows a clearer HL response regarding *LHCX1* gene transcription (but not resolved at the protein level) than the Pt1 strain used in the experiments performed by Nymark et al. (2009) and Bailleul et al. (2010). Although in both strains LHCX1 is the predominant LHCX protein under LL conditions, Pt1 contains higher levels of LHCX1 mRNA and protein (Bailleul et al., 2010), which might limit its ability to increase their amount under HL.

The increase of gene transcripts is often well paralleled by the respective protein changes (Lee et al., 2011; Dyhrman et al., 2012). After 2 h of HL, the huge increase of *LHCX2* and *LHCX3* transcripts was reflected by the respective protein levels. This coincided with a higher Dt concentration, resulting from the deepoxidation of mostly de novo-synthesized Dd. As a consequence of the increase of both Dt and LHCX, a higher NPQ was established. Similar results were also obtained recently in *T. pseudonana* (Zhu and Green, 2010). An important question is how these two enhancers of qE may interact. One hint comes from the finding that the amount of Dt alone is only a weak indicator for the quenching capacity (Lavaud et al., 2004; Schumann et al., 2007; Lepetit et al., 2010). If suitable protein-binding sites are missing, a larger number of Dt molecules can be dissolved in the thylakoid lipids and then do not participate in NPQ (Lepetit et al., 2010). Indeed, the ratio of NPQ to Dt was considerably different in mHL and HL cultures. Moreover, the addition of CHX blocked the increase of NPQ beginning after 30 min of HL treatment. This was also the time when the de novo synthesis of Dd+Dt started. Therefore, it can be assumed that, in order to participate in NPQ, the de novo-synthesized Dt molecules need equivalent amounts of newly synthesized nucleus-encoded pigment-binding proteins. Besides *LHCX1*, *LHCX2*, and *LHCX3*, only four *LHCR* genes are more strongly expressed at HL compared with LL conditions (Nymark et al., 2009). LHCR proteins constitute the PSI antenna in diatoms (Veith et al., 2009; Lepetit et al., 2010). There are indications that LHCX proteins (except LHCX1/FCP6; Beer et al., 2006; Lepetit et al., 2010) appear to be rather weakly associated with the thylakoid membrane or with the classical light-harvesting complexes (Zhu, 2009; Grouneva

et al., 2011), similar to their LHCSR/LI818 relatives in *Chlamydomonas reinhardtii* (Richard et al., 2000). As the amount of Dd+Dt bound to LHCR in PSI remains constant at changing light conditions (Lepetit et al., 2010; Juhas and Büchel, 2012), we hypothesize that de novo-synthesized Dd+Dt molecules bind to the newly synthesized LHCX proteins, conferring a higher NPQ. Interestingly, PsbS, which is responsible for NPQ in land plants, binds no xanthophylls (Dominici et al., 2002; Bonente et al., 2008), while the LHCX-related LHCSR3 in *C. reinhardtii* does (Bonente et al., 2011).

Another peculiarity of our data is the strong difference of NPQ during dark or LL recovery conditions after HL treatment. This difference obviously was not due to photoinhibition, as for both recoveries the light treatment before was identical. It is known that full NPQ recovery in diatoms occurs only at LL conditions but not in darkness (Goss et al., 2006; Grouneva et al., 2009). So far, this effect was related to the Dt epoxidation reaction, which might be limited in darkness due to the chlororespiration driving the buildup of the ΔpH and due to a shortage of NADPH (Jakob et al., 1999; Goss et al., 2006; Grouneva et al., 2009). In our experiments, the epoxidation was not different in LL or darkness. After 4 h of recovery, only a minor amount of Dt was present in the cells (1.1 and 0.5 mol Dt 100 mol^{-1} Chl *a* in samples from LL and darkness, respectively; Fig. 3A). Moreover, the addition of the uncoupler NH_4Cl did not relax the NPQ persisting in the dark. Different from the experiments by Jakob et al. (1999), Goss et al. (2006), and Grouneva et al. (2009) mentioned above, our cultures were longer exposed to HL. Obviously, some part of the NPQ created here relies on other processes, which are independent of Dt. Dt-independent NPQ already has been demonstrated in diatoms and was interpreted to be related to a PSII cycle and/or to a rearrangement of the PSII core (Lavaud et al., 2002b; Eisenstadt et al., 2008).

The Regulation of Xanthophyll Cycle Pigment Synthesis

Our data strongly support the assumption that the redox state of the PQ pool might be the trigger for the HL-induced de novo synthesis of Dd+Dt. The HL plus DCMU treatment, which generates massive amounts of singlet oxygen (Flors et al., 2006), prevented the increase of Dd+Dt, thus excluding a possible triggering role of this ROS, in contrast to its influence on *LHCX* gene expression (see below). However, as by binding to Q_B DCMU blocks the photochemical linear electron flow toward $NADP^+$ (Trebst, 2007), the amount of NADPH, which is required in the early steps of carotenoid biosynthesis (Lohr et al., 2012), might indirectly limit the de novo synthesis of Dd+Dt. In contrast, DBMIB equally reduces linear electron flow by preventing electron flow toward the cytochrome b_6f complex (Trebst, 2007) but induced Dd+Dt de novo synthesis. Hence, an NADPH shortage effect as the actual reason for the differences in Dd+Dt de novo synthesis seems rather unlikely compared with the triggering by the redox state of the PQ pool.

All known enzymes involved in carotenoid synthesis are nucleus encoded, but the carotenoid synthesis itself takes place in the chloroplast (Coesel et al., 2008; Frommolt et al., 2008; Lohr, 2011). The Dd+Dt synthesis was unaffected by the nuclear translation inhibitor CHX; hence, its regulation must occur at the posttranslational stage and most probably in the chloroplast. Additionally, the inhibition of plastid translation also does not reduce Dd+Dt de novo synthesis in HL (Olaizola et al., 1994; Wu et al., 2012). While genes encoding Dd-synthesizing enzymes are up-regulated in diatoms that are shifted from darkness to light with moderate intensity (Coesel et al., 2008), their expression is not further induced in LL-to-HL shift experiments similar to our experimental conditions (Nymark et al., 2009). Thus, the posttranslational regulation of Dd+Dt de novo synthesis seems not to require any newly expressed nucleus- or plastid-encoded factor, which could activate the carotenoid-synthesizing enzyme activity. All these features strongly resemble the situation in the green microalga *Haematococcus pluvialis*, where the HL-induced de novo synthesis of the xanthophyll astaxanthin is triggered by the redox state of the PQ pool via posttranslational regulation (Steinbrenner and Linden, 2003). In contrast to the Dd+Dt synthesis, the effect of CHX illustrates the need for the expression of nucleus-encoded gene(s) during the LL decrease of the Dd+Dt pool size. Contrary to what was proposed by Lohr and Wilhelm (1999), this degradation of Dd+Dt does not result in an increase of the amount of Fx under our experimental conditions; instead, Dd+Dt are probably recycled. This fits with recent results pointing out that Fx is not synthesized from Dd but that both xanthophylls share the same precursor pathway (Dambek et al., 2012).

Another interesting observation was that DTT blocked the deepoxidation effectively only during the first 30 min of HL treatment. Even the addition of supplemental DTT, in order to rule out a reduced efficiency during the treatment, did not restore the full inhibitory effect, although it clearly retarded the synthesis of Dt. So far, no Dt biosynthesis pathway excluding the deepoxidation from Dd has been identified (Lohr, 2011). *P. tricornutum* possesses one violaxanthin deepoxidase (VDE), two violaxanthin deepoxidase-like enzymes (VDL), and one violaxanthin deepoxidase-related enzyme (VDR; Coesel et al., 2008; Bertrand 2010). While the role of VDE is clear, the function of VDL/VDR remains speculative. Studies on *P. tricornutum* mutants containing a reduced amount of VDE indicate that these alternative deepoxidases are involved in Dd-to-Dt conversion (Lavaud et al., 2012). It is possible that during DTT inhibition, VDR and VDL perform the Dd deepoxidation reaction, as they might be less sensitive to DTT than VDE. Corresponding to the xanthophyll cycle pigments, their synthesis might be induced in HL, explaining the absence of Dd deepoxidation in the first 30 min of HL. Indeed, in contrast to the VDE,

the transcription of these alternative deepoxidases is upregulated during a short-term light stress (Nymark et al., 2009).

The Regulation of LHCX Gene Expression

The transcript levels of *LHCX1*, *LHCX2*, and *LHCX3* responded to light in a dose-dependent manner. As conclusively demonstrated, the transcription could be induced in LL conditions via a reduced PQ pool for *LHCX1* and *LHCX2* but not for *LHCX3*. Blocking the gene expression of *LHCX1* and *LHCX2* with DCMU in HL was not possible. As mentioned above, besides keeping the PQ pool oxidized, DCMU creates high amounts of singlet oxygen (Flors et al., 2006), which in plants is the most harmful ROS (Triantaphylidès et al., 2008; Triantaphylidès and Havaux, 2009) and which is able to induce nuclear gene expression (op den Camp et al., 2003; Fischer et al., 2004). We assume that *LHCX1* and *LHCX2* are also induced by singlet oxygen, which superimposes on the effect of the PQ pool redox state. Most likely, *LHCX3* is also strongly induced by ROS, as it exhibited a higher relative induction upon the addition of DCMU than in HL without DCMU (Supplemental Fig. S6). This suggests a photoprotective role of LHCX3 at conditions where the light stress is harsh and is in line with our results, where *LHCX3* was the relatively most strongly transcribed *LHCX* gene only at 2,000 μmol photons m^{-2} s^{-1} light exposure.

LHCX1, *LHCX2*, and *LHCX3* are furthermore upregulated in response to blue light via a cryptochrome-mediated pathway (Coesel et al., 2009). Similarly, promoters in Arabidopsis (*Arabidopsis thaliana*) react to various stimuli (Staneloni et al., 2008). Hence, *LHCX* gene expression is apparently fine-tuned by the light quality (cryptochrome photoreceptor) as well as the light intensity either in situations that generate an imbalance between the photosynthetic light reactions and the Calvin cycle (redox state PQ pool) or during prolonged excess light exposure (i.e. "light stress"; ROS). Importantly, all of these triggers might participate together in the cellular light response, albeit to different extents, as a function of the light conditions.

Which Part of the Electron Transport Chain Generates the Redox Signal?

By applying DCMU or DBMIB, we were able to mimic a LL or HL phenotype, respectively, as has been performed in the green alga *Dunaliella tertiolecta* in the pioneering work by Escoubas et al. (1995). Besides green algae, comparable experiments succeeded in cyanobacteria (Li and Sherman, 2000) and land plants (Karpinski et al., 1997; Pfannschmidt et al., 1999; Tullberg et al., 2000). While, regarding the effects of DBMIB and DCMU, it is clear that the generated signal is related to the redox state of the PQ pool, its exact localization in the plastidic electron transport chain remains ambiguous (Pfannschmidt, 2003). The plastoquinol-oxidizing Qo-site of the cytochrome b_6f complex, which binds plastoquinol, activates state transitions and probably other redox-controlled processes via kinase activation (Zito et al., 1999), but it does not account for all PQ pool redox-dependent processes (Baier and Dietz, 2005). Because in our experiments DCMU inhibited the DBMIB effect in LL, we proved that the binding of DBMIB to the cytochrome b_6f complex alone is not responsible for the redox-mediated response. Moreover, in addition to preventing an increase of Dd+Dt in HL due to the oxidized PQ pool, DCMU also inhibited a decrease in LL. In all light conditions, DCMU fixed the Dd+Dt pool size to its actual status. As at these distinct conditions different degrees of deepoxidation are induced (Fig. 3B), which directly depend on the generated ΔpH (Jakob et al., 2001), one can assume either a chlororespiration or a PSI cyclic electron transfer activity. Both processes would change the redox state of the PQ pool. Therefore, it is tempting to speculate that the PQ pool-mediated signal would need not one but two triggers: one is the redox state of the PQ pool itself, and the second one might be the redox state of Q_A, which works as an on/off switch for the downstream PQ pool redox regulation. Alternatively, Q_B could be involved because binding of DCMU here might inactivate this possible regulatory site, preventing any regulation by the PQ pool. The rate-limiting step in the photosynthetic electron transport chain is the diffusion and the reoxidation of the PQ pool (Haehnel, 1984; Rochaix, 2011). In HL conditions, Q_A should be partially oxidized, while the pool itself is reduced, as long as the light reactions are faster than the enzymatic reactions of the Calvin cycle. As a consequence, the synthesis of Dd+Dt is initiated. In LL conditions, Q_A and the PQ pool are oxidized and the Dd+Dt pool size decreases. As long as Q_A is reduced, which in our experiments was induced by adding DCMU or by the sudden transfer of the cells from HL to darkness (Dijkman and Kroon, 2002; Grouneva et al., 2009), there is neither an increase nor a decrease of the Dd+Dt pool size independent of the oxidation state of the PQ pool.

Why should diatoms have an additional on/off switch within the PSII core? One explanation might be based on the very unusual electron fluxes in diatoms, which are still far from being understood. These include the following: (1) a vivid exchange of electrons between the electron transport chains of chloroplasts and mitochondria (Prihoda et al., 2012); (2) a cyclic electron transfer in PSII (Lavaud et al., 2002b; Onno Feikema et al., 2006; Lavaud et al., 2007); (3) a chlororespiration process that can modify the redox balance of the quinones and of PQ (Jakob et al., 1999; Dijkman and Kroon, 2002; Grouneva et al., 2009; Cruz et al., 2011); and (4) a recombination of Q_A^- and Q_B^- with the oxidized states of the manganese cluster in the PSII core induced by conformational changes (Eisenstadt

et al., 2008). Therefore, an additional switch provided by the acceptor side of PSII (Q_A and Q_B) might help, in combination with the redox state of the PQ pool, to sort the different electron flows and to fine-tune the synthesis of xanthophylls and the transcription of light-responsive genes like *LHCX*, depending on the source of electrons.

CONCLUSION

The redox state of the PQ pool is used as a widespread physiological mechanism in green algae and land plants for signaling within the plastid as well as for retrograde signaling from the plastid to the nucleus (Pfannschmidt, 2003; Baier and Dietz, 2005; Fey et al., 2005; Kleine et al., 2009). To our knowledge, no indications for such signaling processes have been reported before in photosynthetic organisms with secondary plastids. In diatoms, a PQ pool redox regulation and retrograde signaling were regarded as unlikely (Wilhelm et al., 2006), especially when taking into account their complex evolutionary history (Bowler et al., 2010) and the abundance of several light sensors (Depauw et al., 2012), which might partially replace this function. We now have demonstrated that diatoms also use the redox state of the PQ pool to control the light acclimation of the plastid, which includes retrograde signaling to the nucleus to regulate photosynthetic gene expression. As the PQ pool oxidation is the slowest step within the electron transport chain, it is the ideal sensor for redox imbalances. This raises the exciting question of how the redox signal can cross the four membranes of the plastid envelope, which is not yet answered in land plants and green algae, although their plastids possess only two membranes (Kleine et al., 2009). Moreover, as diatoms are evolutionarily and physiologically closely related to other members of the Heterokontophyta, like Phaeophyceae, Chrysophyceae, Xanthophyceae, or Pelagophyceae (Adl et al., 2005), it is tempting to assume that such a mechanism also exists in these groups and might even be a universal feature of photosynthetic organisms.

MATERIALS AND METHODS

Cell Culturing and Light Treatments

Phaeodactylum tricornutum (University of Texas Culture Collection, strain 646, so-called Pt4) was grown in airlift tubes in a day/night rhythm of 16/8 h with a light intensity of 40 μmol photons m^{-2} s^{-1} (LL) at 20°C. Cells were cultured in Provasoli's enriched f/2 seawater medium (Guillard, 1975) using Tropic Marin artificial sea salts (Dr. Biener) at a final concentration of 50% compared with natural seawater. Three days after inoculation, the cultures in their exponential phase of growth were concentrated to 10 mg L^{-1} Chl *a*. They were again acclimated to LL for 1 h before the different experiments were started, and sodium carbonate (4 mM) was added to prevent carbon limitation. Light exposure was provided by four 65-W white light energy-saving lamps (Lexman) adjusted at distinct distances in a custom-made glass cylinder that was continuously cooled by a water bath at 20°C. Cell dispersal was secured by a magnetic stirrer. A long-term experiment started at midnight in darkness. At 8 AM, cells were kept in darkness, exposed to LL, or exposed to 750 μmol photons m^{-2} s^{-1} (mHL) until 12 AM, followed by a further dark cycle of 8 h and a subsequent 1 h darkness or LL/mHL exposure. In a short-term experiment, cells were exposed to 2 h of HL (2,000 μmol photons m^{-2} s^{-1} starting at 12 PM), followed by 4 h of recovery using either LL or darkness, with a subsequent 1h HL treatment. In a third experiment, cells were exposed for 2 h to 100 μmol photons m^{-2} s^{-1} (LL_{100}) only, starting at 12 PM.

Sampling

Samples were taken as indicated in "Results." For HPLC analysis, 400 μL of cell suspension was filtered on a Membrane Isopore Polycarbonate 1.2-μm filter (Millipore) and immediately frozen in liquid nitrogen. Pigments were isolated and analyzed the same day. For RNA and protein analyses, 4 mL of cell suspension was centrifuged 4 min at 4°C and 4,000*g*. The supernatant was discarded, and the cells were resolved in 1 mL of ice-cooled phosphate-buffered saline and centrifuged at 14,000*g* for 1 min. The pellet was frozen in liquid nitrogen and stored at −80°C until further analysis.

Chlorophyll Determination

Chl *a* was extracted using successively 10% methanol and 90% acetone. Its concentration was determined in a spectrophotometer (Hitachi U-5100) according to Jeffrey and Humphrey (1975).

Inhibitor Treatments

DTT (500 μM, in water) was added 15 min before HL exposure. In an alternative experiment, DTT in the same concentration was additionally supplied every 20 min during the HL treatment. CHX (2 μg mL^{-1}, in water) was added 45 min before HL treatment. NH_4Cl (5 mM, in water) was supplemented after 2 h of LL recovery following 2 h of HL treatment. DCMU (10 μM, in ethanol; final concentration of ethanol, 2‰) was added either 10 min before the HL treatment or prior to the recovery period. DBMIB (1 μM, in ethanol; final concentration of ethanol, 0.5‰) was supplied 10 min before starting the LL_{100} exposure.

Chlorophyll Fluorescence Measurements

Chlorophyll fluorescence was measured with a Diving-PAM (Walz) whose optic guide was directly immersed into the algal suspension. Saturating flashes were sent at different time points (see "Results"). As the surrounding light interfered with the measurements, immediately before starting the flash the light was switched off, which was assumed to be fast enough to avoid maximal fluorescence relaxation, in line with previous findings (Havaux et al., 1991). The maximum photosynthetic efficiency of PSII was determined as $(F_m - F_o)/F_m = F_v/F_m$, whereby F_m stands for the maximal fluorescence and F_o for the ground fluorescence in low light acclimated cells, and the effective quantum yield of PSII was determined as F_v'/F_m' in cells exposed to the different light treatments. NPQ was calculated using the Stern-Volmer parameter as $NPQ = F_m/F_m' - 1$. Photoinactivation was determined as $1/F_o - 1/F_m$ according to Park et al. (1995) and He and Chow (2003). It has been shown to well describe photoinactivation also in diatoms (Wu et al., 2011; Campbell and Tyystjärvi, 2012). Here, the value of LL-acclimated cells before starting the HL treatment was taken as 100%. For investigating the optimal concentration of DBMIB, fluorescence kinetics were measured during 5 min of illumination with 2,000 μmol photons m^{-2} s^{-1} with a 2500 Schott white light lamp.

Pigment Analysis

Pigment extraction and HPLC analysis followed the protocol established by Jakob et al. (1999). Samples were analyzed with a Hitachi LaChrom Elite HPLC system equipped with a 10°C-cooled autosampler and a Nucleosil 120-5 C18 column (Macherey-Nagel).

RNA Extraction and LHCX Transcript Level Analysis by Real-Time PCR

RNA was extracted using Trizol (Invitrogen) and the RNeasy Mini kit (Qiagen). Contaminations of DNA were removed with TurboDNAse (Ambion).

An equal amount of RNA was used for all samples to be transcribed into complementary DNA (cDNA) using the QuantiTect reverse transcription kit (Qiagen). Resulting cDNA was diluted 2-fold in nuclease-free water. For real-time PCR analysis, 1 μL of cDNA was used in a 20-μL quantitative PCR assay containing also the primer pairs and GoTaq Mastermix (Promega). A geNorm version 3.5 analysis (Vandesompele et al., 2002) was performed according to the authors' instructions, showing that *18S* and *RPS* were both well suited as endogenous reference genes under the conditions used for growing of the cells (Supplemental Fig. S1). Disadvantageous for *18S* as a reference gene were the lower cycle threshold values compared with *LHCX* genes due to its high abundance (around 14 compared with 20–30 for the *LHCX* genes), leading to a decreased sensitivity for weaker expressed genes. However, when DBMIB and DCMU were supplied, *18S* expression was clearly more stable than *RPS* expression (Supplemental Fig. S2). Therefore, the gene encoding *18S* was chosen as the endogenous reference gene. Primer sequences can be found in Supplemental Table S1. Real-Time PCR was performed on a Stratagene Mx3005P system (Agilent) using a two-step protocol. Samples were measured in triplicate. At the end of each run, melting-curve analysis was applied to confirm the specific amplification of the template and to exclude false-positive fluorescence due to side reactions. Cycle threshold values were obtained by utilizing PCR Miner 3.0 (Zhao and Fernald, 2005). Relative transcript levels were calculated according to Pfaffl et al. (2002) and using the REST software tool.

LHCX Protein Analysis

Protein extraction, western blot, and enhanced chemiluminescence detection followed the protocol described by Coesel et al. (2009) but using 14% lithium dodecyl sulfate-PAGE for protein separation. Anti-LHCSR from *Chlamydomonas reinhardtii* (a kind gift of Dr. Graham Peers, University of California, Berkeley), which was already shown to detect the LHCX proteins in *P. tricornutum* (Bailleul et al., 2010), was applied in a 1:5,000 dilution overnight. Anti-PsbB (CP47; Agrisera) was used as a loading control. Chemiluminescence signals were recorded with the CCD camera LAS4000 (Fujifilm Global).

Supplemental Data

The following materials are available in the online version of this article.

Supplemental Figure S1. geNorm analysis of putative endogenous reference genes.

Supplemental Figure S2. Cycle threshold values of *18S* and *RPS* for the different light and inhibitor treatments.

Supplemental Figure S3. Effective PSII quantum yield and NPQ during the 33-h experiment.

Supplemental Figure S4. Dt versus NPQ relationship in mHL, HL, and HL plus CHX-treated cells.

Supplemental Figure S5. Effects of DBMIB and DCMU on effective PSII quantum yield and NPQ.

Supplemental Figure S6. Relative gene expression levels of *LHCX1*, *LHCX2*, *LHCX3*, and *LHCX4* under HL illumination in the presence or absence of DCMU.

Supplemental Table S1. Primer sequences used for gene expression analysis.

ACKNOWLEDGMENTS

We thank Christian Wilhelm and Lars Dietzel for valuable discussions, Torsten Jakob for help with the HPLC, and Graham Peers for providing the LHCSR antibody.

Received September 21, 2012; accepted November 30, 2012; published December 3, 2012.

LITERATURE CITED

Adl SM, Simpson AGB, Farmer MA, Andersen RA, Anderson OR, Barta JR, Bowser SS, Brugerolle G, Fensome RA, Fredericq S, et al (2005) The new higher level classification of eukaryotes with emphasis on the taxonomy of protists. J Eukaryot Microbiol **52:** 399–451

Allen JF, de Paula WBM, Puthiyaveetil S, Nield J (2011) A structural phylogenetic map for chloroplast photosynthesis. Trends Plant Sci **16:** 645–655

Armbrust EV (2009) The life of diatoms in the world's oceans. Nature **459:** 185–192

Baier M, Dietz KJ (2005) Chloroplasts as source and target of cellular redox regulation: a discussion on chloroplast redox signals in the context of plant physiology. J Exp Bot **56:** 1449–1462

Bailleul B, Rogato A, de Martino A, Coesel S, Cardol P, Bowler C, Falciatore A, Finazzi G (2010) An atypical member of the light-harvesting complex stress-related protein family modulates diatom responses to light. Proc Natl Acad Sci USA **107:** 18214–18219

Beer A, Gundermann K, Beckmann J, Büchel C (2006) Subunit composition and pigmentation of fucoxanthin-chlorophyll proteins in diatoms: evidence for a subunit involved in diadinoxanthin and diatoxanthin binding. Biochemistry **45:** 13046–13053

Bertrand M (2010) Carotenoid biosynthesis in diatoms. Photosynth Res **106:** 89–102

Bonente G, Ballottari M, Truong TB, Morosinotto T, Ahn TK, Fleming GR, Niyogi KK, Bassi R (2011) Analysis of LhcSR3, a protein essential for feedback de-excitation in the green alga *Chlamydomonas reinhardtii*. PLoS Biol **9:** e1000577

Bonente G, Howes BD, Caffarri S, Smulevich G, Bassi R (2008) Interactions between the photosystem II subunit PsbS and xanthophylls studied in vivo and in vitro. J Biol Chem **283:** 8434–8445

Bowler C, Allen AE, Badger JH, Grimwood J, Jabbari K, Kuo A, Maheswari U, Martens C, Maumus F, Otillar RP, et al (2008) The *Phaeodactylum* genome reveals the evolutionary history of diatom genomes. Nature **456:** 239–244

Bowler C, Vardi A, Allen AE (2010) Oceanographic and biogeochemical insights from diatom genomes. Annu Rev Mar Sci **2:** 333–365

Brunet C, Lavaud J (2010) Can the xanthophyll cycle help extract the essence of the microalgal functional response to a variable light environment? J Plankton Res **32:** 1609–1617

Campbell DA, Tyystjärvi E (2012) Parameterization of photosystem II photoinactivation and repair. Biochim Biophys Acta **1817:** 258–265

Caron L, Berkaloff C, Duval JC, Jupin H (1987) Chlorophyll fluorescence transients from the diatom *Phaeodactylum tricornutum*: relative rates of cyclic phosphorylation and chlororespiration. Photosynth Res **11:** 131–139

Coesel S, Mangogna M, Ishikawa T, Heijde M, Rogato A, Finazzi G, Todo T, Bowler C, Falciatore A (2009) Diatom PtCPF1 is a new cryptochrome/photolyase family member with DNA repair and transcription regulation activity. EMBO Rep **10:** 655–661

Coesel S, Oborník M, Varela J, Falciatore A, Bowler C (2008) Evolutionary origins and functions of the carotenoid biosynthetic pathway in marine diatoms. PLoS ONE **3:** e2896

Cruz S, Goss R, Wilhelm C, Leegood R, Horton P, Jakob T (2011) Impact of chlororespiration on non-photochemical quenching of chlorophyll fluorescence and on the regulation of the diadinoxanthin cycle in the diatom *Thalassiosira pseudonana*. J Exp Bot **62:** 509–519

Dambek M, Eilers U, Breitenbach J, Steiger S, Büchel C, Sandmann G (2012) Biosynthesis of fucoxanthin and diadinoxanthin and function of initial pathway genes in *Phaeodactylum tricornutum*. J Exp Bot **63:** 5607–5612

Depauw FA, Rogato A, Ribera d'Alcalá M, Falciatore A (2012) Exploring the molecular basis of responses to light in marine diatoms. J Exp Bot **63:** 1575–1591

Dijkman NA, Kroon BMA (2002) Indications for chlororespiration in relation to light regime in the marine diatom *Thalassiosira weissflogii*. J Photochem Photobiol B **66:** 179–187

Dominici P, Caffarri S, Armenante F, Ceoldo S, Crimi M, Bassi R (2002) Biochemical properties of the PsbS subunit of photosystem II either purified from chloroplast or recombinant. J Biol Chem **277:** 22750–22758

Dyhrman ST, Jenkins BD, Rynearson TA, Saito MA, Mercier ML, Alexander H, Whitney LP, Drzewianowski A, Bulygin VV, Bertrand EM, et al (2012) The transcriptome and proteome of the diatom Thalassiosira pseudonana reveal a diverse phosphorus stress response. PLoS ONE **7:** e33768

Eisenstadt D, Ohad I, Keren N, Kaplan A (2008) Changes in the photosynthetic reaction centre II in the diatom Phaeodactylum tricornutum

result in non-photochemical fluorescence quenching. Environ Microbiol **10:** 1997–2007

Engelken J, Funk C, Adamska I (2012) The extended light-harvesting complex (LHC) protein superfamily: classification and evolutionary dynamics. *In* R Burnap, W Vermaas, eds, Functional Genomics and Evolution of Photosynthetic Systems, Vol 33. Springer, New York, pp 265–284

Escoubas JM, Lomas M, LaRoche J, Falkowski PG (1995) Light intensity regulation of cab gene transcription is signaled by the redox state of the plastoquinone pool. Proc Natl Acad Sci USA **92:** 10237–10241

Fey V, Wagner R, Bräutigam K, Pfannschmidt T (2005) Photosynthetic redox control of nuclear gene expression. J Exp Bot **56:** 1491–1498

Fischer BB, Krieger-Liszkay A, Eggen RL (2004) Photosensitizers neutral red (type I) and rose bengal (type II) cause light-dependent toxicity in *Chlamydomonas reinhardtii* and induce the Gpxh gene via increased singlet oxygen formation. Environ Sci Technol **38:** 6307–6313

Flors C, Fryer MJ, Waring J, Reeder B, Bechtold U, Mullineaux PM, Nonell S, Wilson MT, Baker NR (2006) Imaging the production of singlet oxygen in vivo using a new fluorescent sensor, Singlet Oxygen Sensor Green. J Exp Bot **57:** 1725–1734

Foyer CH, Neukermans J, Queval G, Noctor G, Harbinson J (2012) Photosynthetic control of electron transport and the regulation of gene expression. J Exp Bot **63:** 1637–1661

Frommolt R, Werner S, Paulsen H, Goss R, Wilhelm C, Zauner S, Maier UG, Grossman AR, Bhattacharya D, Lohr M (2008) Ancient recruitment by chromists of green algal genes encoding enzymes for carotenoid biosynthesis. Mol Biol Evol **25:** 2653–2667

Geider RJ, Delucia EH, Falkowski PG, Finzi AC, Grime JP, Grace J, Kana TM, La Roche J, Long SP, Osborne BA, et al (2001) Primary productivity of planet Earth: biological determinants and physical constraints in terrestrial and aquatic habitats. Glob Change Biol **7:** 849–882

Goss R, Jakob T (2010) Regulation and function of xanthophyll cycle-dependent photoprotection in algae. Photosynth Res **106:** 103–122

Goss R, Ann Pinto E, Wilhelm C, Richter M (2006) The importance of a highly active and DeltapH-regulated diatoxanthin epoxidase for the regulation of the PS II antenna function in diadinoxanthin cycle containing algae. J Plant Physiol **163:** 1008–1021

Green BR (2011) Chloroplast genomes of photosynthetic eukaryotes. Plant J **66:** 34–44

Grouneva I, Jakob T, Wilhelm C, Goss R (2009) The regulation of xanthophyll cycle activity and of non-photochemical fluorescence quenching by two alternative electron flows in the diatoms *Phaeodactylum tricornutum* and *Cyclotella meneghiniana*. Biochim Biophys Acta **1787:** 929–938

Grouneva I, Rokka A, Aro EM (2011) The thylakoid membrane proteome of two marine diatoms outlines both diatom-specific and species-specific features of the photosynthetic machinery. J Proteome Res **10:** 5338–5353

Guillard RRL (1975) Culture of phytoplankton for feeding marine invertebrates. *In* WL Smith, MH Chaney, eds, Culture of Marine Invertebrate Animals. Plenum, New York, 29–60

Haehnel W (1984) Photosynthetic electron transport in higher plants. Annu Rev Plant Physiol **35:** 659–693

Havaux M, Strasser RJ, Greppin H (1991) A theoretical and experimental analysis of the qP and qN coefficients of chlorophyll fluorescence quenching and their relation to photochemical and nonphotochemical events. Photosynth Res **27:** 41–55

He J, Chow WS (2003) The rate coefficient of repair of photosystem II after photoinactivation. Physiol Plant **118:** 297–304

Jahns P, Holzwarth AR (2012) The role of the xanthophyll cycle and of lutein in photoprotection of photosystem II. Biochim Biophys Acta **1817:** 182–193

Jakob T, Goss R, Wilhelm C (1999) Activation of diadinoxanthin de-epoxidase due to a chlororespiratory proton gradient in the dark in the diatom *Phaeodactylum tricornutum*. Plant Biol **1:** 76–82

Jakob T, Goss R, Wilhelm C (2001) Unusual pH-dependence of diadinoxanthin de-epoxidase activation causes chlororespiratory induced accumulation of diatoxanthin in the diatom *Phaeodactylum tricornutum*. J Plant Physiol **158:** 383–390

Jeffrey SW, Humphrey GF (1975) New spectrophotometric equations for determining chlorophylls a, b, c1 and c2 in higher plants, algae and natural phytoplankton. Biochem Physiol Pflanzen **167:** 191–194

Juhas M, Büchel C (2012) Properties of photosystem I antenna protein complexes of the diatom *Cyclotella meneghiniana*. J Exp Bot **63:** 3673–3681

Karpinski S, Escobar C, Karpinska B, Creissen G, Mullineaux PM (1997) Photosynthetic electron transport regulates the expression of cytosolic ascorbate peroxidase genes in *Arabidopsis* during excess light stress. Plant Cell **9:** 627–640

Kikutani S, Tanaka R, Yamazaki Y, Hara S, Hisabori T, Kroth PG, Matsuda Y (2012) Redox regulation of carbonic anhydrases via thioredoxin in chloroplast of the marine diatom *Phaeodactylum tricornutum*. J Biol Chem **287:** 20689–20700

Kleine T, Voigt C, Leister D (2009) Plastid signalling to the nucleus: messengers still lost in the mists? Trends Genet **25:** 185–192

Kroth PG, Chiovitti A, Gruber A, Martin-Jezequel V, Mock T, Parker MS, Stanley MS, Kaplan A, Caron L, Weber T, et al (2008) A model for carbohydrate metabolism in the diatom *Phaeodactylum tricornutum* deduced from comparative whole genome analysis. PLoS ONE **3:** e1426

Kurisu G, Zhang H, Smith JL, Cramer WA (2003) Structure of the cytochrome b6f complex of oxygenic photosynthesis: tuning the cavity. Science **302:** 1009–1014

Lavaud J (2007) Fast regulation of photosynthesis in diatoms: mechanisms, evolution and ecophysiology. Funct Plant Sci Biotech **1:** 267–287

Lavaud J, Materna AC, Sturm S, Vugrinec S, Kroth PG (2012) Silencing of the violaxanthin de-epoxidase gene in the diatom *Phaeodactylum tricornutum* reduces diatoxanthin synthesis and non-photochemical quenching. PLoS ONE **7:** e36806

Lavaud J, Rousseau B, Etienne AL (2004) General features of photoprotection by energy dissipation in planktonic diatoms (Bacillariophyceae). J Phycol **40:** 130–137

Lavaud J, Rousseau B, van Gorkom HJ, Etienne AL (2002a) Influence of the diadinoxanthin pool size on photoprotection in the marine planktonic diatom *Phaeodactylum tricornutum*. Plant Physiol **129:** 1398–1406

Lavaud J, Strzepek RF, Kroth PG (2007) Photoprotection capacity differs among diatoms: possible consequences on the spatial distribution of diatoms related to fluctuations in the underwater light climate. Limnol Oceanogr **52:** 1188–1194

Lavaud J, van Gorkom HJ, Etienne AL (2002b) Photosystem II electron transfer cycle and chlororespiration in planktonic diatoms. Photosynth Res **74:** 51–59

Lee MV, Topper SE, Hubler SL, Hose J, Wenger CD, Coon JJ, Gasch AP (2011) A dynamic model of proteome changes reveals new roles for transcript alteration in yeast. Mol Syst Biol **7:** 514

Lepetit B, Goss R, Jakob T, Wilhelm C (2012) Molecular dynamics of the diatom thylakoid membrane under different light conditions. Photosynth Res **111:** 245–257

Lepetit B, Volke D, Gilbert M, Wilhelm C, Goss R (2010) Evidence for the existence of one antenna-associated, lipid-dissolved and two protein-bound pools of diadinoxanthin cycle pigments in diatoms. Plant Physiol **154:** 1905–1920

Li H, Sherman LA (2000) A redox-responsive regulator of photosynthesis gene expression in the cyanobacterium *Synechocystis* sp. strain PCC 6803. J Bacteriol **182:** 4268–4277

Li Z, Wakao S, Fischer BB, Niyogi KK (2009) Sensing and responding to excess light. Annu Rev Plant Biol **60:** 239–260

Lohr M (2011) Carotenoid metabolism in phytoplankton. *In* S Roy, CA Llewellyn, E Skarstadt Egeland, G Johnsen, eds, Phytoplankton Pigments: Characterization, Chemotaxonomy and Applications in Oceanography. Cambridge University Press, New York, pp 113–161

Lohr M, Schwender J, Polle JEW (2012) Isoprenoid biosynthesis in eukaryotic phototrophs: a spotlight on algae. Plant Sci **185−186:** 9–22

Lohr M, Wilhelm C (1999) Algae displaying the diadinoxanthin cycle also possess the violaxanthin cycle. Proc Natl Acad Sci USA **96:** 8784–8789

Long SP, Humphries S, Falkowski PG (1994) Photoinhibition of photosynthesis in nature. Annu Rev Plant Physiol Plant Mol Biol **45:** 633–662

Materna A, Sturm S, Kroth PG, Lavaud J (2009) First induced plastid genome mutations in an alga with secondary plastids: *psbA* mutations in the diatom *Phaeodactylum tricornutum* (Bacillariophyceae) reveal consequences on the regulation of photosynthesis. J Phycol **45:** 838–846

Nymark M, Valle KC, Brembu T, Hancke K, Winge P, Andresen K, Johnsen G, Bones AM (2009) An integrated analysis of molecular acclimation to high light in the marine diatom *Phaeodactylum tricornutum*. PLoS ONE **4:** e7743

Obrig TG, Culp WJ, McKeehan WL, Hardesty B (1971) The mechanism by which cycloheximide and related glutarimide antibiotics inhibit peptide synthesis on reticulocyte ribosomes. J Biol Chem **246:** 174–181

Olaizola M, LaRoche J, Kolber Z, Falkowski PG (1994) Non-photochemical fluorescence quenching and the diadinoxanthin cycle in a marine diatom. Photosynth Res **41:** 357–370

Onno Feikema W, Marosvölgyi MA, Lavaud J, van Gorkom HJ (2006) Cyclic electron transfer in photosystem II in the marine diatom *Phaeodactylum tricornutum*. Biochim Biophys Acta **1757:** 829–834

op den Camp RGL, Przybyla D, Ochsenbein C, Laloi C, Kim C, Danon A, Wagner D, Hideg E, Göbel C, Feussner I, et al (2003) Rapid induction of distinct stress responses after the release of singlet oxygen in *Arabidopsis*. Plant Cell **15:** 2320–2332

Oudot-Le Secq M-P, Grimwood J, Shapiro H, Armbrust EV, Bowler C, Green BR (2007) Chloroplast genomes of the diatoms *Phaeodactylum tricornutum* and *Thalassiosira pseudonana*: comparison with other plastid genomes of the red lineage. Mol Genet Genomics **277:** 427–439

Park YI, Chow WS, Anderson JM (1995) Light inactivation of functional photosystem II in leaves of peas grown in moderate light depends on photon exposure. Planta **196:** 401–411

Pfaffl MW, Horgan GW, Dempfle L (2002) Relative Expression Software Tool (REST) for group-wise comparison and statistical analysis of relative expression results in real-time PCR. Nucleic Acids Res **30:** e36

Pfannschmidt T (2003) Chloroplast redox signals: how photosynthesis controls its own genes. Trends Plant Sci **8:** 33–41

Pfannschmidt T (2010) Plastidial retrograde signalling: a true "plastid factor" or just metabolite signatures? Trends Plant Sci **15:** 427–435

Pfannschmidt T, Nilsson A, Allen JF (1999) Photosynthetic control of chloroplast gene expression. Nature **397:** 625–628

Prihoda J, Tanaka A, de Paula WBM, Allen JF, Tirichine L, Bowler C (2012) Chloroplast-mitochondria cross-talk in diatoms. J Exp Bot **63:** 1543–1557

Richard C, Ouellet H, Guertin M (2000) Characterization of the LI818 polypeptide from the green unicellular alga *Chlamydomonas reinhardtii*. Plant Mol Biol **42:** 303–316

Rochaix JD (2011) Regulation of photosynthetic electron transport. Biochim Biophys Acta **1807:** 375–383

Ruban AV, Johnson MP, Duffy CDP (2012) The photoprotective molecular switch in the photosystem II antenna. Biochim Biophys Acta **1817:** 167–181

Ruban AV, Lavaud J, Rousseau B, Guglielmi G, Horton P, Etienne AL (2004) The super-excess energy dissipation in diatom algae: comparative analysis with higher plants. Photosynth Res **82:** 165–175

Schumann A, Goss R, Jakob T, Wilhelm C (2007) Investigation of the quenching efficiency of diatoxanthin in cells of *Phaeodactylum tricornutum* (Bacillariophyceae) with different pool sizes of xanthophyll cycle pigments. Phycologia **46:** 113–117

Setkov NA, Kazakov VN, Rosenwald IB, Makarova GF, Epifanova OI (1992) Protein synthesis inhibitors, like growth factors, may render resting 3T3 cells competent for DNA synthesis: a radioautographic and cell fusion study. Cell Prolif **25:** 181–191

Staneloni RJ, Rodriguez-Batiller MJ, Casal JJ (2008) Abscisic acid, high-light, and oxidative stress down-regulate a photosynthetic gene via a promoter motif not involved in phytochrome-mediated transcriptional regulation. Mol Plant **1:** 75–83

Steinbrenner J, Linden H (2003) Light induction of carotenoid biosynthesis genes in the green alga *Haematococcus pluvialis*: regulation by photosynthetic redox control. Plant Mol Biol **52:** 343–356

Strzepek RF, Harrison PJ (2004) Photosynthetic architecture differs in coastal and oceanic diatoms. Nature **431:** 689–692

Tirichine L, Bowler C (2011) Decoding algal genomes: tracing back the history of photosynthetic life on Earth. Plant J **66:** 45–57

Trebst A (2007) Inhibitors in the functional dissection of the photosynthetic electron transport system. Photosynth Res **92:** 217–224

Triantaphylidès C, Havaux M (2009) Singlet oxygen in plants: production, detoxification and signaling. Trends Plant Sci **14:** 219–228

Triantaphylidès C, Krischke M, Hoeberichts FA, Ksas B, Gresser G, Havaux M, Van Breusegem F, Mueller MJ (2008) Singlet oxygen is the major reactive oxygen species involved in photooxidative damage to plants. Plant Physiol **148:** 960–968

Tullberg A, Alexciev K, Pfannschmidt T, Allen JF (2000) Photosynthetic electron flow regulates transcription of the psaB gene in pea (*Pisum sativum* L.) chloroplasts through the redox state of the plastoquinone pool. Plant Cell Physiol **41:** 1045–1054

Vandesompele J, De Preter K, Pattyn F, Poppe B, Van Roy N, De Paepe A, Speleman F (2002) Accurate normalization of real-time quantitative RT-PCR data by geometric averaging of multiple internal control genes. Genome Biol **3:** 0034.1

Veith T, Brauns J, Weisheit W, Mittag M, Büchel C (2009) Identification of a specific fucoxanthin-chlorophyll protein in the light harvesting complex of photosystem I in the diatom *Cyclotella meneghiniana*. Biochim Biophys Acta **1787:** 905–912

Vener AV, van Kan PJ, Rich PR, Ohad I, Andersson B (1997) Plastoquinol at the quinol oxidation site of reduced cytochrome bf mediates signal transduction between light and protein phosphorylation: thylakoid protein kinase deactivation by a single-turnover flash. Proc Natl Acad Sci USA **94:** 1585–1590

Wilhelm C, Büchel C, Fisahn J, Goss R, Jakob T, Laroche J, Lavaud J, Lohr M, Riebesell U, Stehfest K, et al (2006) The regulation of carbon and nutrient assimilation in diatoms is significantly different from green algae. Protist **157:** 91–124

Wu H, Cockshutt AM, McCarthy A, Campbell DA (2011) Distinctive photosystem II photoinactivation and protein dynamics in marine diatoms. Plant Physiol **156:** 2184–2195

Wu H, Roy S, Alami M, Green BR, Campbell DA (2012) Photosystem II photoinactivation, repair, and protection in marine centric diatoms. Plant Physiol **160:** 464–476

Yamamoto HY, Kamite L (1972) The effects of dithiothreitol on violaxanthin de-epoxidation and absorbance changes in the 500-nm region. Biochim Biophys Acta **267:** 538–543

Zhao S, Fernald RD (2005) Comprehensive algorithm for quantitative real-time polymerase chain reaction. J Comput Biol **12:** 1047–1064

Zhu SH (2009) Characterization of LI818-like genes under various stress conditions in the marine diatom *Thalassiosira pseudonana*. PhD thesis. University of British Columbia, Vancouver

Zhu SH, Green BR (2008) Light harvesting and photoprotection in diatoms: identification and expression of LI818-like proteins. *In* JF Allen, E Gantt, JH Golbeck, B Osmond, eds, Energy from the Sun. Springer, New York, pp 261–264

Zhu SH, Green BR (2010) Photoprotection in the diatom *Thalassiosira pseudonana*: role of LI818-like proteins in response to high light stress. Biochim Biophys Acta **1797:** 1449–1457

Zito F, Finazzi G, Delosme R, Nitschke W, Picot D, Wollman FA (1999) The Qo site of cytochrome b6f complexes controls the activation of the LHCII kinase. EMBO J **18:** 2961–2969